

PRELIMINARY DESIGN OF PINHOLE CAMERA FOR NSLS-II PROJECT*

I. Pinayev[#], B. Kosciuk, O. Singh, BNL, Upton, NY 11973, U.S.A.

Abstract

The NSLS-II Light Source being built at Brookhaven National Laboratory is expected to provide very small emittances and electron beam sizes. High resolution imaging systems are required in order to provide robust measurements. The pinhole camera will utilize 6-fold magnification with a pinhole placed inside a crotch absorber. The pinhole is protected from high power synchrotron radiation with a filter made of refractory metal. In this paper we provide resolution analyses, heat load calculations, and optimization details for the NSLS-II pinhole camera, including beamline design.

INTRODUCTION

The pinhole camera has been a workhorse for measuring electron beam size on the storage ring-based light sources since it was first utilized at ESRF [1]. The NSLS-II storage ring will utilize diffraction limited electron beam size in the vertical plane [2] in order to achieve unprecedented brightness. The goal of the study described in this paper is to define the resolution of the imaging system and optimize beamline design. Initially, the storage ring will have only three damping wigglers installed and commissioning will be performed without the damping wigglers. In the final configuration eight damping wigglers are planned. The pinhole camera is expected to operate with a circulating current from 5 to 500 mA. The electron beam sizes corresponding to these

conditions are shown in Table 1.

Table 1: Electron Beam Parameters for Different Number of Damping Wigglers

	$\epsilon, \text{ nm}$	σ_E/E	σ, μ
Horizontal plane without damping wigglers	2.06	0.05%	125.1
Horizontal plane with 3 damping wigglers	0.9	0.09%	163.9
Horizontal plane with 8 damping wigglers	0.5	0.1%	175.0
Vertical plane	0.008	0.05-0.1%	12.4-13.4

BEAMLINE LAYOUT

The expected layout of the pinhole camera beamline is shown in Fig. 1. The bending dipoles of the storage ring have a low magnetic field of 0.4 T in order to reach small horizontal emittance [2]. Therefore, the expected critical energy of the dipole synchrotron radiation is rather low, namely 2.4 keV. In order to improve resolution by utilizing shorter wavelength we will employ a three-pole wiggler as a source. The field of the central pole is 1.14 T and the critical photon energy is 6 keV and the useful synchrotron radiation spectrum extends to 50 keV. The electron beam parameters at the location of the three-pole

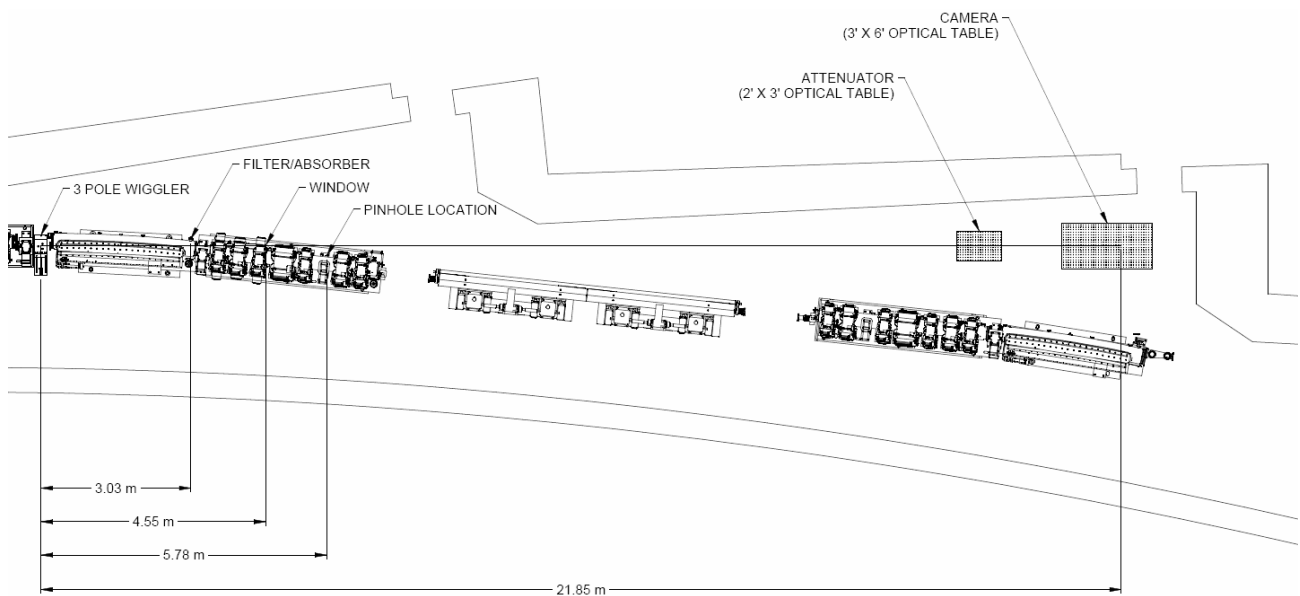


Figure 1: Layout of three-pole wiggler pinhole camera. In the baseline design the pinhole is placed inside absorber the alternative location in indicated. Nominal pinhole camera magnification slightly exceeds 6.

*Work supported by U.S. Department of Energy, Office of Science, Office of Basic Energy Sciences, under Contract DE-AC02-98CH10886.

[#]pinayev@bnl.gov

wiggler are $\eta_x=0.17$ m, $\beta_x=4.1$ m, and $\beta_y=19.3$ m. Taking emittances $\epsilon_x=0.9$ nm and $\epsilon_y=8$ pm and the relative energy spread $\sigma_E/E=0.1\%$ one can easily find transverse sizes of the source $\sigma_x=180$ microns (defined mostly by energy spread) and $\sigma_y=12.4$ microns.

The first element of the pinhole beamline is the molybdenum filter/attenuator. It constitutes a 200 μ foil mounted inside of a crotch absorber in order to remove low-energy photons. Its purpose is to decrease the heat load on the downstream elements to acceptable level and to improve the resolution of the pinhole camera. Molybdenum as material was chosen for its high melting temperature and high heat conduction. The thickness of the foil was a compromise between temperature rise of the foil (which is cooled by conduction) and sufficient flux of the X-ray photons. The simulated temperature distribution is shown in Fig. 2.

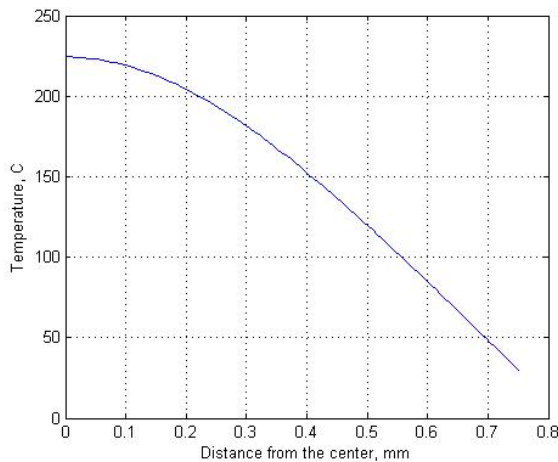


Figure 2: Temperature distribution of molybdenum foil. Heat load was approximated by Gaussian shape with peak density of 30 W/mm² and rms width of 0.24 mm. The foil is mounted over a 1.5 mm slot in a water-cooled absorber.

The filter is followed by a pinhole mounted on the same absorber, as shown in Fig. 3.

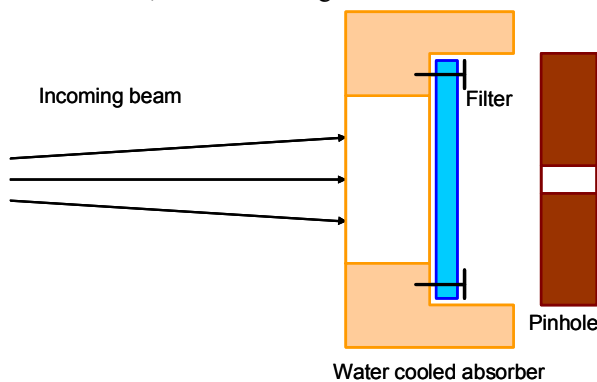


Figure 3: Placement of the pinhole inside the absorber.

The aluminum window with 500 microns thickness provides sufficient mechanical strength and has substantial transmission above 10 keV. Because all low energy photons are absorbed by the filter the peak thermal

load on the window is about 12 mW/mm². The image of the electron beam will be observed with CdWO₄ phosphor and camera, equipped with a zoom lens.

RESOLUTION ESTIMATION

Use of the molybdenum filter concentrates the spectrum around 20 keV (see Fig. 4).

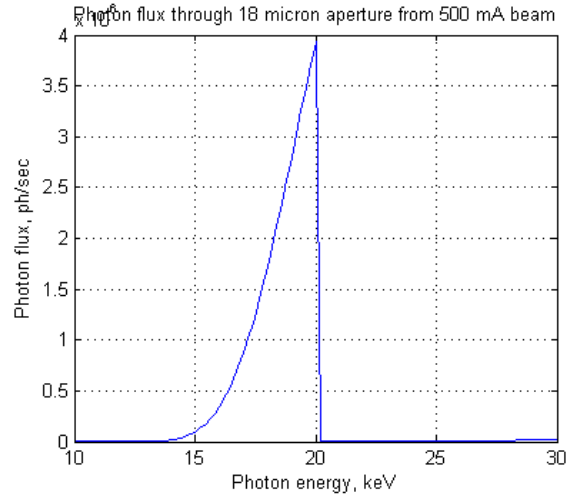


Figure 4: X-ray photons flux after 18 microns aperture located at 3.03 m from the three-pole wiggler. The beam intensity was attenuated by 200-micron molybdenum foil, a 0.5 mm aluminum window, and 17 meters of air path.

In the dedicated MATLAB® script numerical integration was performed over a spectral range from 10 to 30 keV in order to estimate photons density on the phosphor screen. For each particular wavelength the number of photons passed through the pinhole was found and photon density in the image plane was calculated using a Gaussian curve in which width corresponds to resolution estimated using the approach in [3]. The point spread function was found by summing over all wavelengths and was fitted with the Gaussian curve. The resultant rms width was used as the resolution of the system.

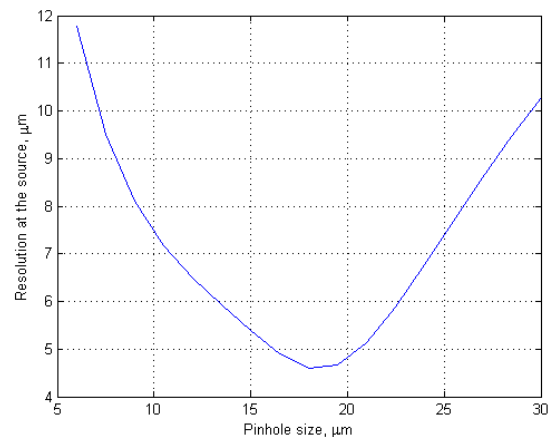


Figure 5: Dependence of pinhole camera resolution on aperture size for in vacuum placement of the pinhole.

In order to optimize the design the described procedure was applied the set of pinhole sizes. The curve for calculated resolution dependence on the pinhole size is shown in Fig. 5. The best resolution of 4.6 microns is achieved with a pinhole size of about 18 microns.

The proposed design makes the pinhole camera suitable for measuring of the beam vertical size. Due to the magnification resolution of the imaging system is of less concern as well. However, there are certain technical difficulties, such as provisions for adjusting the pinhole, which need to be overcome.

Alternatively the pinhole can be installed after the aluminum window. Putting the pinhole assembly outside the vacuum chamber simplifies design and service of the beamline but sacrifices achievable resolution. The distance from the pinhole to the source is defined by the available physical space and is expected to be approximately 6 meters (see Fig. 1).

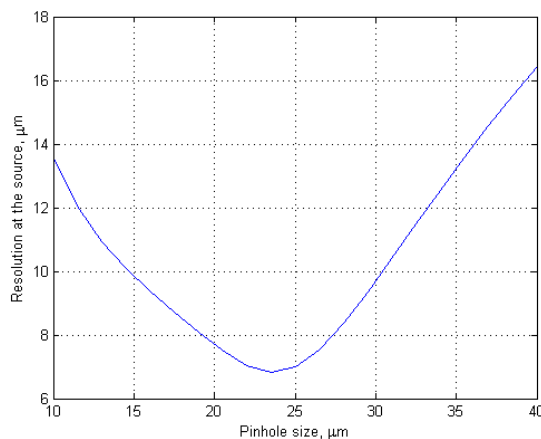


Figure 6: Resolution of the pinhole camera with in-air pinhole.

The alternative design provides resolution of 7 microns with an optimal pinhole size of 23 microns. The image beam size on the phosphor screen is expected to be at least 30 microns (for the in-air pinhole) and therefore phosphor resolution (6-10 μ [4]) should not affect the accuracy of measurements. In any case the real beam size will be found using the deconvolution with calculated point spread function of the system.

CONCLUSIONS

The pinhole camera planned for installation on the NSLS-II storage ring provides sufficient resolution for robust measurement of vertical beam size if positioned inside a crotch absorber of dipole vacuum chamber. Being placed outside of vacuum chamber the camera has marginal resolution but can be a useful tool for monitoring fluctuations of beam size during regular operations.

The resolution in the horizontal plane is quite adequate in both cases and the camera can be a very useful for monitoring of beam energy spread, which defines the beam size at the location of the three-pole wiggler.

REFERENCES

- [1] P. Elleaume et al., *J. Synchrotron Rad.* (1995). 2, 209-214.
- [2] S. Ozaki et al., *Philosophy for NSLS-II design with sub-nanometer horizontal emittance*, PAC'07, pp. 77-79 (2007)
- [3] B. Yang, "Optical System Design for High-Energy Particle Beam Diagnostics," *BIW'02*, AIP Proc. 648, 2002, pp.59-78
- [4] C.A. Thomas, G. Rehm, "Pinhole Camera Resolution and Emittance Measurement," *EPAC'08*, pp. 1254-1256.